

1 **Supplementary information**

2 **Supplementary Methods**

3 *Chemicals and metabolites.* DMXAA (Selleck S1537), HT-DNA (Sigma), 2'3'-cGAMP (Invivogen
4 1441190), Digitonin (Sigma D5628), 2-DG (Selleck S4701), Oxamate (Selleck S6871), AOA (Selleck
5 S4989), FHIN (GLP BIO GC32878), DEBM (Sigma 112038), DMM (Sigma 136441), Oligomycin
6 (Selleck S1478), Rotenone (Selleck S2348), Piericidin A (Cayman 15379), BPTES (Selleck S7753),
7 Rapamycin (Selleck S1039), Metformin (Selleck S1950), Dimethyl D-(+)-Malate (TCI, M1347),
8 Dimethyl α -ketoglutarate (Sigma, 349631), Succinate (TCI, S0104), MMF (TCI, S2413), Arginine
9 (Sigma A5006), Citrulline (Sigma C7629), ASA (Argino-succinate) (Sigma A5707), Thymidine (Sigma
10 T1895), ddC (Absin abs811894), VBIT-4 (Selleck S3544), Oxaliplatin (Selleck S1224), Gemcitabine
11 (Selleck S1149), Necrostatin-1 (Selleck S8037), GSK'872 (Selleck S8465).

12

13 *Cell culture, HT-DNA transfection and DMXAA stimulation.* L929 cells, BJ-5ta and RAW264.7 cells
14 were purchased from the ATCC. B16-F10 cells and MC38 cells were contributed by laboratory of M.
15 Luo. HT-1080 and LLC cells were obtained from the Cell Bank of the Chinese Academy of Sciences.
16 These cell lines were grown in DMEM (Meilunbio) containing 10% FBS (Gibco), penicillin (100 U/ml)
17 and streptomycin (100 μ g/ml). All cells were maintained at 37 °C and 5% CO₂ and were tested for
18 mycoplasma. Cells were seeded in 6-well plate and HT-DNA was transfected into cells using
19 Lipofectamine 2000 (Thermo Fisher) at a concentration of 0.5 μ g/ml. Cells were treated with DMXAA
20 at a concentration of 50 μ M.

21

22 *RNAi.* Cells were seeded at equal densities and grown to confluency over a period of 24 h. Opti-
23 MEM and lipofectamine RNAiMax (Thermo) were used for reverse transfection of short interfering
24 RNA (siRNA) for 48h. The siGOT2 (5'-GCCTTCACTATGGTCTGCAA-3') and siGPT2 (5'-
25 CGGCATTTCTACGATCCTGAA-3') were used in this study.

26

27 *Quantitative real-time PCR (qRT-PCR).* Cells were cultured as mentioned above and total RNA was
28 collected in lysis buffer (EZBioscience) and extracted using EZ-press RNA Purification Kit (B0004D)
29 according to the manufacturer's instructions. RNA was subjected to cDNA synthesis using 4× EZscript
30 Reverse Transcription Mix II (with gDNA Remover) (EZB-RT2GQ). The cDNA was diluted 10 times
31 and then performed the real-time qPCR reaction containing SYBR ChamQ Universal SYBR qPCR
32 Master Mix (Vazyme) and gene-specific primers listed in Supplemental Table S1. The reactions were
33 performed in a QuantStudio™ 6 Flex Real-Time PCR System (Applied Biosystems).

34 *Generation of knockdown cell pools.* The shRNA sequences targeting *Cad*, *Vdac1/3*, *Ripk1*, *Ripk3*
35 and *Mkl1* were ligated into the plko.1 vector. The shRNA construct was co-transfected with packaging
36 (psPAX2) and envelope (pMD2.G) vectors into HEK293T cells. Lentivirus from supernatant was
37 harvested at 24h and then mixed with 8µg/ml polybrene to infect L929 cells. The stable cells were
38 selected in 10ug/ml puromycin for 2 days.

39

40 *CRISPR-cas9 mediated gene knockout.* sgRNA sequences targeting mouse cGAS, STING, IRF3,
41 ZBP1, BAX and BAK listed in TableS2 were ligated into plasmid lentiCRISPRv2 (Addgene, deposited
42 by Feng Zhang of MIT) digested by Bsmbl (NEB). The construct was packaged into a lentivirus. L929
43 cells were then infected with lentivirus and selected in 10ug/ml puromycin for 2 days.

44

45 *Western Blot.* Cells were cultured in six-well plates under the indicated treatment conditions. After
46 treatment, the culture medium was discarded, and cells were washed with cold PBS. Cells were then
47 lysed with SDS sample loading buffer and boiled at 95 °C for 8 min. Protein samples were separated
48 by SDS-PAGE and transferred onto NC membranes. The membranes were blocked with skim milk
49 at room temperature for 1 h and subsequently incubated with primary (1:1000) and secondary (1:500)
50 antibodies. The immunoreacted products were visualized using ECL reagent and autoradiography by
51 GE Typhoon FLA 9500. Primary antibody lists : STING (D2P2F) (Cell Signaling Cat# 13647) TBK1
52 (Cell Signaling Cat# 3504) IRF3 (Cell Signaling Cat# 4302) p-TBK1(Ser172) (D52C2) (Cell Signaling
53 Cat# 5483) p-IRF3(Ser396) (D6O1M) (Cell Signaling Cat# 29047) Actin (Proteintech Cat# 66009-1)
54 TOM20 (Novus Cat# NBP1-81556) Gapdh (6C5) (Santa Cruz Cat# sc-32233) Histone H3 (Cell

55 Signaling Cat# 9715S) Bax (Cell Signaling Cat# 2772) Bak (D4E4) (Cell Signaling Cat# 12105) Stat1
56 (Cell Signaling Cat# 14994) p-Stat1 (58D6) (Cell Signaling Cat# 9167) Zbp1 (Adipogen Cat# AG-20B-
57 0010) RIP (D94C12) (Cell Signaling Cat# 3493) RIP3 (D4G2A) (Cell Signaling Cat# 95702) MLKL
58 (E7V4W) (Cell Signaling Cat# 37705).

59

60 *Co-immunoprecipitation.* The cytosolic fraction was obtained by lysing the cells with NP-40 lysis buffer
61 (Beyotime). Protein A agarose beads (Millipore 16125) and IRF3, RIPK1/RIPK3 antibodies were used
62 for co-IP from cytosolic fractions. 20 μ L of sample was mixed with 2 \times SDS sample loading buffer and
63 boiled at 95°C for 8 minutes. The samples were loaded on SDS-PAGE gels for electrophoresis.

64

65 *Cellular immunofluorescence.* BJ-5ta cells were fixed in 4% Paraformaldehyde (Servicbio) for 10min
66 at room temperature followed by 3 x 5 minute washes in PBS. Then cells were permeabilized with
67 0.1% (v/v) Triton X-100 in PBS for 10 minutes at room temperature followed by 3 x 5 minute washes
68 in PBS and blocked in 3% BSA for an hour. Cells were then incubated with corresponding primary
69 antibodies overnight at 4°C. Cells were washed 3 x 5 minute washes in PBS and incubated with
70 secondary antibody for an hour at room temperature followed by 3 x 5 minute washes. To visualize
71 the nuclei, cells were co-stained with DAPI (Sigma D9542). Immunofluorescence pictures were taken
72 by Leica SP8 laser scanning confocal microscope and analyzed by Image J. Primary antibody list:
73 DNA (Millipore #CBL186), TOM20 (Novus Cat# NBP1-81556) IRF3 (D614C) (Cell Signaling Cat#
74 11904).

75 *NADH/NAD ratio detection.* NAD⁺ levels were determined by using NAD⁺/NADH assay kit with WST-
76 8 (Beyotime) according to the manufacturer's instructions. In brief, about 1 \times 10⁶ cells were added 200
77 μ L of NAD⁺/NADH extraction solution with a gently pipette, then centrifuged at 12,000g at 4°C for 10
78 minutes. Supernatant was transferred to a 96-well plate as the sample to measure total NAD⁺ and
79 NADH. 50-100 μ L of the sample was heated for 30 minutes in a 60°C water bath and 20 μ L supernatant
80 was transferred to a 96-well plate as the sample to measure NADH. After adding the alcohol
81 dehydrogenase working solution, samples were incubated at 37°C in the dark for 10 minutes. Then
82 added chromogenic solution to each well and incubated at 37°C in the dark for 30 minutes.

83 Absorbance at 450 nm was measured and analyzed on a plate reader (BioTek).

84 *SIM-Ultimate two-color imaging.* Cells were pretreated with AOA for 6 hours, or with 5 μ M ABT-737
85 and 1 μ M S63845 (Selleck) for 20 minutes. Subsequently, the cells were incubated in DMEM
86 containing SYBR Gold (10,000 \times) and PK Orange (1,000 \times) for 15 minutes. After staining, cells were
87 washed three times with PBS and imaged at 37 °C in a humidified incubator with 5% CO₂ using an
88 Olympus SIM-Ultimate microscope.

89

90 *Apoptotic cell death analysis.* Apoptotic cell death was assessed by flow cytometry with FITC-Annexin
91 V (Vazyme, Cat# A211-02) and live/dead (Fixable Viability Stain 780, BD Biosciences, catalog no.
92 565388). The dilution of the staining reagents was performed according to the manufacturer's
93 instructions.

94

95 *cGAMP Detection.* MC38 tumor cells were treated with gemcitabine or oxaliplatin in 6-well plate, and
96 cultured for 24 hours. Then cells were collected and lysed using MPER™ Mammalian Protein
97 Extraction Reagent (Thermo Scientific, Cat# 78503) at 4°C for 20 min. Then cGAMP in cell lysates
98 was determined using 2'3'-cGAMP ELISA Kit (Cayman Chemical, Cat# 501700) according to
99 standard protocols.

100

101 *IFN-beta and CXCL10 measurement by ELISA.* Cytokine levels in mouse serum were measured with
102 Mouse IFN-beta Quantikine ELISA Kit (Bio-techne) and Mouse IP-10 ELISA Kit (CXCL10) (Abcam)
103 according to the manufacturer's instructions.

104

105 *Immunohistochemistry.* The tissue specimens were fixed overnight in 10% formalin and then were
106 dehydrated in increasing concentrations of ethanol, followed by clearing of alcohol by xylene. The
107 specimens were subsequently embedded in paraffin wax and sectioned continuously at a thickness
108 of 4 μ m. Hematoxylin and eosin (H&E) staining was performed according to standard protocols. For

109 immunohistochemistry, the sections were deparaffinized with xylene for 15 min three times and
110 rehydrated in 100%, 85% and 75% ethanol for 5 min. Then, tissue sections were incubated in citrate
111 buffer for antigen retrieval. The sections were then placed into 3% hydrogen peroxide and incubated
112 at room temperature for 25 min to block endogenous peroxidase activity. After three times washing,
113 tissue sections were blocked with 3% BSA for 30min at room temperature and stained with primary
114 antibodies including anti-CD3 (GB111337), anti-CD8 (GB12068) and anti-granzyme B (GB12092)
115 and incubated at 4°C overnight. The sections were then incubated with HRP-conjugated secondary
116 antibodies at room temperature for 1 h. After three washes with PBS, DAB solution (G1211,
117 Servicebio) was added and the slides were counterstained with hematoxylin.

118

119 *[U-13C]-aspartate tracing analysis.* Samples were analyzed by Q Exactive quadrupole orbitrap high
120 resolution mass spectrometry coupled with a Dionex Ultimate 3000 RSLC (HPG) ultra-performance
121 liquid chromatography (UPLC-Q-Orbitrap-HRMS) system (Thermo Fisher Scientific), with a HESI
122 ionization source. The injection volume was 2 μ L. Samples were separated with an ACQUITY UPLC
123 BEH Amide column (100 mm \times 2.1 mm, 1.7- μ m particle size; Waters). The mobile phase consisted
124 of 25 mM ammonium formate and 20 mM ammonium hydroxide in water (A), and acetonitrile (B), the
125 gradient elution was set as follows: 0–1.0 min, 95% B; 1.0–11.0 min, 95%–45% B; 11.0–12.0 min,
126 45% B; 12.1–17 min, 95% B. The flow rate was 0.3mL/min and column temperature 45°C.

127 All MS experiments were performed in positive and negative ion modes using a heated ESI
128 source. The source and ion transfer parameters applied were as followed: spray voltage 3.5 kV
129 (positive) 2.8kV (negative). For the ionization mode, the sheath gas, aux gas, capillary temperature
130 and heater temperature were maintained at 40, 10 (arbitrary units), 320 °C and 350 °C, respectively.
131 The S-Lens RF level was set at 50. The Orbitrap mass analyzer was operated at a resolving power
132 of 70,000 in full-scan mode (scan range: 200-1200 m/z; automatic gain control (AGC) target: 1e6)
133 and of 17,500 in the Top 3 data-dependent MS2 mode (stepped normalized collision energy: 10, 20
134 and 30; injection time: 50 ms; isolation window: 1.2 m/z; AGC target: 1e5) with a dynamic exclusion
135 setting of 5.0 seconds.

136

137 *Cytosolic mtDNA/mtRNA extraction and detection.* As described in Supplementary Figure 7A, 5×10^6
138 L929 cells were equally divided into two aliquots. One aliquot was boiled with 50 mM NaOH at 95°C
139 for 30 min followed by adding 1 M Tris-HCl (pH 8.0) to neutralize the pH and then centrifuged at 12000
140 g for 10 min. Another aliquot was resuspended in 300µL buffer containing 50 mM HEPES (pH 7.4),
141 150 mM NaCl and 20µg/mL digitonin. The resuspensions were incubated at 4°C for 10 min to allow
142 plasma membrane permeabilization and then centrifuged at 980 g for 3 min three times. The cytosolic
143 supernatants were centrifuged at 12000 g for 10 min to avoid remaining cellular debris, yielding
144 cytosolic preparations free of nuclear, mitochondrial and endoplasmic reticulum contamination. DNA
145 was then purified from these pure cytosolic fractions using TIANamp Genomic DNA Kit (TIANGEN).
146 Quantitative real-time PCR was performed for both whole-cell extracts and cytosolic fractions using
147 nuclear DNA primers (*Tert*) and mtDNA primers (*Dloop1-3*, *Cytb*, *ND1* and *ND4*), and the Ct values
148 obtained for mtDNA abundance for whole-cell extracts served as normalization controls for the mtDNA
149 values determined from the cytosolic fractions. To determine the presence of mtRNA in the cytosol,
150 qPCR was performed using primers specific for mitochondrial D-loop on cDNA, which had been
151 reverse-transcribed from RNA isolated from the cytosolic fraction (mtRNA).

152

153 *END-seq library preparation.* END-seq was performed according to a previously described protocol(1).
154 Briefly, L929 cells were treated as mentioned above. About 10 million cells were embedded in agarose
155 plugs and subjected to protein and RNA digestion. The DNA within the plugs was blunted, A-tailed
156 and ligated with a biotin-labelled hairpin adaptor. Subsequently, the agarose plugs were melted, and
157 DNA was extracted and sheared by sonication. After C1 bead purification, the DNA fragments were
158 ligated to a second adaptor and amplified for sequencing with Illumina sequencing primers.

159 *Bioinformatics analysis.* The genome-wide transcriptome data quantified as fragments per kilobase
160 per million were downloaded from TCGA. We used the data from 12 cancer types, all of which had
161 profiled enough numbers of samples for both cancer and normal tissues. Data include Bladder
162 Urothelial Carcinoma (BLCA), Breast Cancer (BRCA), Colon Adenocarcinoma (COAD), Esophageal
163 Carcinoma (ESCA), Head and Neck Squamous Cell Carcinoma (HNSC), kidney clear cell carcinoma
164 (KIRC), lung adenocarcinoma (LUAD), Lung Squamous Cell Carcinoma (LUSC), Mesothelioma

165 (MESO), Ovarian Cancer (OV), rectum adenocarcinoma (READ) and Uterine Corpus Endometrial
166 Carcinoma (UCEC). We identified and evaluated the levels of immune infiltrates of CD8⁺ T cell by the
167 Tumor immune estimation resource (TIMER) algorithm, which is a resource for systematic estimation
168 of the abundances of six immune cell types (B cell, CD4⁺ T cell, CD8⁺ T cell, neutrophil, macrophage
169 and dendritic cell) by using transcriptome profile(2). We characterized the overall activity of the
170 aspartate/pyrimidine synthesis pathway by calculating the average expression of genes involved in
171 this pathway in each tumor sample including GOT2, GPT2, CAD, DHODH, and UMPS. The Pearson
172 correlation analysis was performed to determine the associations between aspartate/pyrimidine
173 synthesis activity and CD8⁺ T cell fraction.

174

175 **References**

176

- 177 1. Canela A, Sridharan S, Sciascia N, Tubbs A, Meltzer P, Sleckman BP, et al. DNA Breaks and
178 End Resection Measured Genome-wide by End Sequencing. *Mol Cell*. 2016;63(5):898-911.
- 179 2. Li T, Fu J, Zeng Z, Cohen D, Li J, Chen Q, et al. TIMER2.0 for analysis of tumor-infiltrating
180 immune cells. *Nucleic Acids Res*. 2020;48(W1):W509-W14.

181

182

183

184

185

186

187

188

189 **Supplemental Figure Legends**

190 **Supplemental Figure 1. The aminotransferase inhibitor AOA induces and enhances ISGs in**
191 **cells.**

192 **(A)** MC38 cells were treated with inhibitors from (Figure 1A) followed by 0.5µg/ml HT-DNA transfection
193 for 6h, cells were harvested for qPCR analysis of *Ifnb*. **(B-D)** RAW264.7 (mouse macrophage cell
194 line), HT-1080 (human fibrosarcoma cell line), B16-F10 (mouse melanoma cell line) were treated with
195 0.5mM AOA and/or HT-DNA (0.5µg/ml) for 6 h, cells were harvested for qPCR analysis of ISGs
196 expression. **(E-G)** Secreted IFN-β protein levels in culture supernatants were measured by ELISA.
197 **(H-J)** Western blot detected P-IRF3, P-TBK1 levels in different cell line treated as indicated. **(K)**
198 Western blot analysis in L929 cell monoclonal transduced with the indicated gene-specific guide RNA
199 (gRNA) or scrambled (Scr) gRNA control to determine the knockout efficiency. **(L)** cGAS-KO/STING-
200 KO/IRF3-KO L929 cell lines were treated with 0.5 mM AOA and/or HT-DNA (0.5µg/ml) for 6 h, cells
201 were harvested for qPCR analysis of ISGs expression. **(M-O)** *Rigi* or *Ifih1* knockdown MC38 cells
202 were treated with AOA and/or HT-DNA for 6 h, followed by qPCR analysis of *Rigi* **(M)** or *Ifih1* **(N)**
203 knockdown efficiency and ISGs expression **(O)**. Data are represented as means ± SEM.
204 Representative data are shown from two or three independent experiments. Statistical analysis was
205 performed by unpaired *t* test **(B-G, O)** and 1-way ANOVA **(M, N)** or 2-way ANOVA **(L)** followed by
206 Tukey's test. **P* < 0.05; ***P* < 0.01; ****P* < 0.001; *****P* < 0.0001.

207

208 **Supplemental Figure 2. Co-depletion of GOT2 and GPT2 slightly induced ISG expression and**
209 **exhibited amplification of DNA-stimulated ISG expression.**

210 **(A and B)** The relative *IFNB* and *CXCL10* mRNA expression in the control BJ-5ta cells versus *GOT1*

211 siRNA-silencing BJ-5ta cells (A) or *GOT2* siRNA-silencing BJ-5ta cells (B). (C) The relative *GPT2*
212 mRNA expression in the control BJ-5ta cells versus *GOT2* siRNA-silencing BJ-5ta cells. (D) The
213 relative *IFNB* and *CXCL10* mRNA expression in the control BJ-5ta cells versus *GPT2* siRNA-silencing
214 BJ-5ta cells. (E) The relative ISG expression in the control MC38 cells versus *Gpt2* knockdown MC38
215 cells after indicated treatment. (F) The relative ISG expression in the control MC38 cells versus *Got2*
216 and *Gpt2* double knockdown MC38 cells after indicated treatment. (G) Western blot detected P-IRF3,
217 P-STAT1, GOT2 and GPT2 levels in MC38 cells treated as in (F). (H and I) Relative *IFNB* mRNA
218 levels (H) and effector protein expression (I) in control BJ-5ta cells and BJ-5ta cells with *GPT2/GOT2*
219 double knockdown following the indicated treatments. Data are represented as means \pm SEM.
220 Representative data are shown from two or three independent experiments. Statistical analysis was
221 performed by unpaired *t* test (A-F) or 2-way ANOVA followed by Tukey's test (H).

222

223 **Supplemental Figure 3. Aspartate deficiency augments cGAS-STING-mediated type I**
224 **interferon response.**

225 (A) Relative aspartate and asparagine levels in L929 cells pre-treated with 0.5 mM AOA for 1 h
226 followed by HT-DNA (0.5 μ g/ml) transfection for 6 h or not compared with Mock group (n=3). (B)
227 Relative aspartate levels in L929 cells after indicated treatment compared with Mock (shScr) group.
228 (C-G) BJ-5ta, HT-1080, RAW264.7, B16-F10 and MC38 cells were treated with 0.5 mM AOA for 1 h
229 followed by DMXAA (50 μ M) stimulation or HT-DNA (0.5 μ g/ml) transfection or not for 6 h in the absence
230 or presence of 20 mM aspartate, and then cells were harvested for qPCR analysis of IFN response
231 gene expression. (H) KEGG pathways enrichment of the up-regulated genes. (I-M) Western blot
232 detected P-IRF3, P-TBK1 levels in different cell lines treated as in C-G. Data are represented as

233 means \pm SEM. Representative data are shown from two or three independent experiments. Statistical
234 analysis was performed by unpaired *t* test (**A**) or 1-way ANOVA followed by Tukey's test (**B-G**). **P* <
235 0.05; ***P* < 0.01; ****P* < 0.001; *****P* < 0.0001.

236

237 **Supplemental Figure 4. The effect of AOA on enhancing ISGs cannot be reversed by most of**
238 **examined metabolites.**

239 (**A**) Relative abundances of metabolites in TCA and urea cycle were measured in L929 cells treated
240 as indicated by LC-MS. (**B-E**) BJ-5ta were treated with or without 1mM AOA for 1 h followed by HT-
241 DNA (0.5 μ g/ml) stimulation for 6 h in the absence or presence of indicated metabolites, and then cells
242 were harvested for qPCR analysis of type I IFN expression. (**F-J**) L929 cells were treated with or
243 without 0.5 mM AOA for 1 h followed by HT-DNA (0.5 μ g/ml) stimulation for 6 h in the absence or
244 presence of indicated metabolites, and then cells were harvested for qPCR analysis of *Cxcl10*
245 expression. (**K**) A schematic representation showing AOA induced ROS production and imbalanced
246 NAD⁺/NADH ratio. (**L**) Intracellular NAD⁺/NADH ratio were measured by NAD⁺/NADH detection kit.
247 L929 cells were treated as indicated. (**M**) L929 were treated with 0.5 mM AOA for 1 h followed by HT-
248 DNA (0.5 μ g/ml) transfection for 6 h in the absence or presence of NAC (N-acetylcysteine), and then
249 cells were harvested for qPCR analysis of ISGs expression. Data are represented as means \pm SEM.
250 Representative data are shown from two or three independent experiments. Statistical analysis was
251 performed by unpaired *t* test (**A**) or 1-way ANOVA followed by Tukey's or Bonferroni's test (**B-M**). **P*
252 < 0.05; ***P* < 0.01; ****P* < 0.001; *****P* < 0.0001.

253

254 **Supplemental Figure 5. The effect of AOA on enhancing ISG expression is hindered by**

255 **pyrimidine nucleosides.**

256 **(A and B)** L929 **(A)** or MC38 **(B)** cells were treated with 0.5 mM AOA for 1 h followed by HT-DNA (0.5
257 µg/ml) stimulation for 6 h in the absence or presence of pyrimidine nucleosides (+100µM, ++200µM
258 cytidine, thymidine and uridine), and then cells were harvested for qPCR analysis of ISGs expression.
259 **(C)** Verifying *Cad* knockdown efficiency by qPCR in L929 cells. Data are represented as means ±
260 SEM. Representative data are shown from two or three independent experiments. Statistical analysis
261 was performed by 1-way ANOVA followed by Tukey's test **(A-C)**. **P* < 0.05; ***P* < 0.01; ****P* < 0.001;
262 *****P* < 0.0001.

263

264 **Supplemental Figure 6. The effect of AOA on enhancing ISG expression is not associated with**
265 **DNA damage or cell apoptosis.**

266 **(A and B)** Western blot detected γH2AX and P-IRF3 levels in L929 **(A)** and BJ-5ta cells **(B)** treated
267 as indicated. **(C)** MC38 cells were treated with AOA for 6 h, followed by collection of whole-cell lysates
268 (WCL) or isolation of mitochondrial (Mito) and nuclear (Nuc) fractions. Western blot validation of
269 subcellular fractionation. **(D-F)** Mass spectrometry analysis of relative aspartate levels in WCL **(D)**,
270 mitochondrial **(E)**, and nuclear fractions **(F)** (n=3). **(G)** Western blot analysis of BAX and BAK in L929
271 cells to determine the knockout efficiency. **(H)** *Bax* and *Bak* knockout L929 cells were treated with 0.5
272 mM AOA and/or HT-DNA (0.5µg/ml) for 6 h, cells were harvested for qPCR analysis ISGs expression.
273 **(I and J)** Representative flow cytometric images **(I)** and quantitative analysis **(J)** of the percentage of
274 FVS780⁺Annexin V⁺ cells in L929 cells treated with different dose of AOA. Representative data are
275 shown from two independent experiments. Statistical analysis was performed by unpaired *t* test **(D-**
276 **F)** or 1-way ANOVA followed by Tukey's test **(H and J)**. **P* < 0.05; ***P* < 0.01; ****P* < 0.001; *****P* <

277 0.0001.

278

279 **Supplemental Figure 7. AOA triggers mtDNA release to amplify cGAS-STING activation.**

280 (A) Schematic of the subcellular fractionation protocol. (B) Western blot detected α -Tubulin (cytosol),
281 TOM20 (OMM), PDH (Matrix), COX IV (IMM) and Histone H3 (nuclei) to validate pure cytosolic
282 fraction in MC38 cells treated as indicated. (C) MC38 cells were treated with AOA in the absence or
283 presence of 20mM aspartate followed by HT-DNA transfection and then cells were harvested for
284 qPCR analysis of mtDNA levels in cytosolic fractions. (D and E) MC38 cells (D) or L929 cells (E) were
285 treated with AOA in the absence or presence of 20 mM aspartate and then cells were harvested for
286 qPCR analysis of mtDNA levels in cytosol. (F and G) The relative cytosolic mtDNA levels in *Got2* and
287 *Gpt2* shRNA-silencing and control MC38 cells (F) or siRNA-silencing and control L929 cells (G). (H)
288 Relative mtDNA copy number of wild-type MC38 cells exposed to ddC for 7 days. (I) ISGs expression
289 were analyzed by qPCR after indicated treatment. Representative data are shown from two or three
290 independent experiments. (J) MC38 cells were treated AOA for 6 h, followed by qPCR analysis of
291 mtRNA levels in cytosolic fractions. Statistical analysis was performed by unpaired *t* test (F-H, J) and
292 1-way ANOVA (C-E) or 2-way ANOVA (I) followed by Tukey's test. **P* < 0.05; ***P* < 0.01; ****P* < 0.001;
293 *****P* < 0.0001.

294

295 **Supplemental Figure 8. Aspartate deficiency enhances cGAS-STING signaling through VDAC-**
296 **mediated mtDNA release.**

297 (A) Representative Immunofluorescence images of mitochondrial (TOM20, red) or dsDNA (green) in
298 BJ-5ta cells treated with AOA in the absence or presence of VBIT-4 for 6 h. Scale bars, 10 μ m. Right:

299 quantification of cytosolic dsDNA in BJ-5ta cells with indicated treatment (n=48 fields per group from
300 3 biological replicates). (B) L929 cells were treated with 10 μ M VBIT-4 (inhibitor of voltage-dependent
301 anion channel (VDAC) oligomerization) for 48 h and then treated with AOA and/or HT-DNA for 6 h.
302 Cells were harvested for qPCR analysis of ISGs expression. (C) Scr and *Vdac1/3* knockdown L929
303 cells were treated as indicated, followed qPCR analysis of ISGs expression. (D and E) L929 cells (D)
304 and MC38 cells (E) were treated as indicated, P-IRF3 and P-STAT1 levels were detected by western
305 blot. (F and G) MC38 cells (F) and B16-F10 cells (G) were treated with 10 μ M VBIT-4 for 48 h and
306 then treated with AOA and/or HT-DNA for 6 h. ISGs expression were analyzed by qPCR.
307 Representative data are shown from two or three independent experiments. Statistical analysis was
308 performed by 1-way ANOVA (A, B, F, G) or 2-way ANOVA (C) followed by Tukey's test. * $P < 0.05$; ** P
309 < 0.01 ; *** $P < 0.001$; **** $P < 0.0001$.

310

311 **Supplemental Figure 9. The strengthening effect of mtDNA on the cGAS-STING pathway is**
312 **independent of MLKL-mediated necroptotic signaling.**

313 (A and B) qPCR analysis (A) and western blots (B) of Scr and *Zbp1*^{-/-} L929 cells with indicated
314 treatment. (C) L929 cells were treated with Necrostatin-1 (Nec-1, 10 mM) or GSK'872 (2.5 mM) for
315 48h, followed by HT-DNA stimulation for 6 hrs with or without AOA for qPCR analysis. (D)
316 Endogenous colP in L929 cells with indicated treatment. (E and F) qPCR analysis (E) and western
317 blots (F) of Scr and *Mlkl*-knockdown L929 cells with indicated treatment. Data are represented as
318 means \pm SEM. Representative data are shown from two or three independent experiments. Statistical
319 analysis was performed by 2-way ANOVA followed by Tukey's test (A, C and E). * $P < 0.05$; ** $P < 0.01$;
320 *** $P < 0.001$; **** $P < 0.0001$.

321

322 **Supplemental Figure 10. AOA augments the effect of cGAMP on inducing type I IFN responses.**

323 **(A-C)** Body weight of animals in Figure 6. **(D)** Gating strategies of FACS. **(E and F)** AOA enhances
324 cGAMP-mediated antitumor response. Quantification analysis of the percentage of CD8⁺ T cells in
325 living cells and surface CD69 expression **(E)**, IFN γ and TNF α production **(F)** on CD8⁺ T cells isolated
326 from tumors of B16-F10 tumor bearing mice. FACS analysis was performed on day 14 after
327 inoculation with 2×10^5 tumor cells (n=7-9). Data are represented as means \pm SEM. Representative
328 data are shown from two or three independent experiments. Statistical analysis was performed by
329 unpaired t test **(E and F)**. *P < 0.05; **P < 0.01; ***P < 0.001; ****P < 0.0001.

330

331 **Supplemental Figure 11. AOA does not directly alter CD8⁺ T cell metabolism or function**

332 **(A-C)** C57BL/6 mice were intraperitoneally injected with PBS or AOA (5 mg/kg) for 18 h, followed by
333 FACS sorting of splenic CD8⁺ T cells for metabolomic analysis. Schematic of the experimental design
334 **(A)**, heatmap of metabolite changes in CD8⁺ T cells (n=3) **(B)** and relative aspartate levels in CD8⁺ T
335 cells **(C)**. **(D-I)** CD8⁺ T cells were sorted from spleens of C57BL/6 mice and treated in vitro with AOA
336 (1 mM) for 1 h followed by cGAMP (5 μ M) stimulation for 6 h, then subjected to metabolomic or FACS
337 analysis. Schematic of the experimental design **(D)**, heatmap of metabolite changes in CD8⁺ T
338 cells(n=3) **(E)** and relative aspartate levels in CD8⁺ T cells **(F)**. FACS analysis of CD69 **(G)**, IFN γ **(H)**,
339 and TNF α **(I)** expression in CD8⁺ T cells. Data are represented as means \pm SEM. Representative data
340 are shown from two or three independent experiments. Statistical analysis was performed by unpaired
341 t test **(C and F, G-I)**. *P < 0.05; **P < 0.01; ***P < 0.001; ****P < 0.0001.

342

343 **Supplemental Figure 12. AOA enhances CD8⁺ T cell responses through type I interferon**
344 **signaling**

345 **(A–D)** CD8⁺ T cells were sorted from spleens of C57BL/6 mice and cultured in MC38-derived
346 conditioned medium for 24 h, followed by FACS analysis. Schematic of the experimental design **(A)**.
347 ELISA quantification of IFN β in MC38-derived conditioned medium **(B)**. FACS analysis of CD69
348 expression **(C)** and IFN γ production **(D)** in CD8⁺ T cells. **(E and F)** Tumor volume **(E)** and Kaplan–
349 Meier survival curves **(F)** of C57BL/6 mice inoculated with 8×10^5 MC38 cells (n = 6). Mice received
350 anti-CD8 antibody (10 mg/kg, i.p.) or isotype control on days 0, 3, 6, 9, and 12 and were treated with
351 cGAMP (3 μ g/mouse) combined with AOA (5 mg/kg, i.p.) or PBS on days 7, 10, and 13. **(G and H)**
352 Tumor volume **(G)** and Kaplan–Meier survival curves **(H)** of *Ifnar1*-KO C57BL/6 mice inoculated with
353 8×10^5 MC38 cells (n = 6). Mice were treated with cGAMP (3 μ g/mouse) combined with AOA (5 mg/kg,
354 i.p.) or PBS on days 7, 10, and 13. **(I and J)** Tumor volume **(I)** and Kaplan–Meier survival curves **(J)**
355 of C57BL/6 mice inoculated with 8×10^5 MC38 cells (n = 6). Mice received 20mg/kg of anti-IFNAR1
356 antibody or isotype control intraperitoneally on days 0, 3, 6, 9, and 12 and were treated with cGAMP
357 (3 μ g/mouse) combined with AOA (5 mg/kg, i.p.) or PBS on days 7, 10, and 13. Data are represented
358 as means \pm SEM. Representative data are shown from two or three independent experiments.
359 Statistical analysis was performed by 1-way ANOVA **(B–D)** and 2-way ANOVA followed by Tukey’s test
360 **(E, G, I)** or log-rank test **(F, H and J)**. *P < 0.05; **P < 0.01; ***P < 0.001; ****P < 0.0001.

361

362 **Supplemental Figure 13. AOA synergizes with chemotherapy-mediated antitumor immunity in**
363 **the AOM/DSS CRC model**

364 **(A)** Schematic of the AOM/DSS-induced CRC mouse model, treated with oxaliplatin or/and AOA.
365 Oxaliplatin was administered every 4 days combined with daily injections of AOA for four injections.
366 **(B)** Body weight dynamics of AOM/DSS-induced murine colorectal cancer model. **(C and D)**
367 Representative colon images **(C)** and tumor number **(D)**. Scale bars, 1 cm. **(E and F)** CD8⁺ T cells
368 producing IFN γ **(E)** and TNF α **(F)** in the lamina propria were analyzed on day 85 after AOM injection
369 (n = 6 per group). Data are represented as means \pm SEM. Representative data are shown from two
370 or three independent experiments. Statistical analysis was performed by 1-way ANOVA followed by
371 Bonferroni's test **(D-F)**. *P < 0.05; **P < 0.01; ***P < 0.001; ****P < 0.0001.

372

373 **Supplemental Figure 14. AOA synergizes with radiotherapy to enhance ISG induction and**
374 **suppress tumor growth**

375 **(A)** MC38 cells were irradiated with 6 Gy and treated with AOA for 24 or 48 h, followed by qPCR
376 analysis of *Irfn*b and ISGs. **(B and C)** Tumor volume **(B)** and Kaplan–Meier survival curves **(C)** of
377 C57BL/6 mice inoculated with 8×10^5 MC38 cells (n = 6). Mice received 6 Gy irradiation on days 11,
378 14, and 17 and daily AOA (5 mg/kg, i.p.) or PBS from days 11 to 19. **(D)** Body weight of mice in **(B)**.
379 Data are represented as means \pm SEM. Representative data are shown from two or three
380 independent experiments. Statistical analysis was performed by unpaired *t* test **(B and D)** or 1-way
381 ANOVA followed by Tukey's test **(A)** and log-rank test **(C)**. *P < 0.05; **P < 0.01; ***P < 0.001; ****P
382 < 0.0001.

383 **Supplemental Figure 15. Lower aspartate correlates with enhanced anti-tumor immunity in**
384 **cancer patients**

385 **(A)** Correlation analysis for aspartate-related pyrimidine synthesis pathway activity score level versus
386 cGAS, STING1, IRF3 and ISG15 in human KIRC, KIRP and LIHC from TCGA Pan Cancer Atlas. R
387 and P represent Pearson's correlation coefficients and 2-tailed P values. Abbreviation: KIRC (n = 524),
388 Kidney renal clear cell carcinoma; KIRP (n = 284), Kidney renal papillary cell carcinoma; LIHC (n =
389 363), Liver hepatocellular carcinoma. **(B)** The correlation analysis of aspartate-related pyrimidine
390 synthesis pathway activity score with CD8⁺ T cell infiltration for TCGA cancer type. Each red line
391 represents a regression line with Spearman's correlation coefficient (R). Abbreviation: BLCA (n = 404),
392 Bladder Urothelial Carcinoma; BRCA (n = 1058), Breast invasive carcinoma; COAD (n = 435), Colon
393 adenocarcinoma; ESCA (n = 152), Esophageal carcinoma; HNSC (n = 494), Head and Neck
394 squamous cell carcinoma; KIRC (n = 524), Kidney renal clear cell carcinoma; LUAD (n = 497), Lung
395 adenocarcinoma; LUSC (n = 489), Lung squamous cell carcinoma; MESO (n = 80), Mesothelioma;
396 OV (n = 353), Ovarian serous cystadenocarcinoma; READ (n = 156), Rectum adenocarcinoma;
397 UCEC (n = 536), Uterine Corpus Endometrial Carcinoma; **(C)** LC-MS analysis of aspartate in human
398 colorectal tumor tissue (CRC, n = 20 patients). **(D)** Representative IHC and H&E staining of tumor
399 tissue in human colorectal carcinomas, showing lymphocyte cell infiltration and pathology. Scale bars,
400 200µm. **(E)** The correlations of aspartate levels with CD3, CD8 or granzyme B expression in colorectal
401 tumor tissue (CRC, n = 20 patients). **(F)** Diagram showing that intracellular aspartate deficiency blocks
402 the CAD-mediated *de novo* pyrimidine synthesis pathway, resulting in the release of mitochondrial
403 DNA (mtDNA), which amplifies cGAS-STING pathway response to agonists via the ZBP1-RIPK1/3
404 axis.

Table S1: List of primers used in qPCR

Gene	Forward Sequence	Reverse Sequence
Mouse-Actb	ATGCTCCCCGGGCTGTAT	CATAGGAGTCCTTCTGACCCAT TC
Mouse-Ifnb	TCCGAGCAGAGATCTTCAGGAA	TGCAACCACCACTCATTCTGAG
Mouse-Cxcl10	GCCGTCATTTTCTGCCTCA	CGTCCTTGCAGAGGGGATC
Mouse-Ccl5	ACGTCAAGGAGTATTTCTACAC	GATGTATTCTTGAACCCACT
Mouse-Isg15	CATCCTGGTGAGGAACGAAAGG	CTCAGCCAGAACTGGTCTTCGT
Mouse-lfi44	CTGATTACAAAAGAAGACATGACA GAC	AGGCAAACCAAAGACTCCA
Mouse-Usp18	GAGAGGACCATGAAGAGGA	TAAACCAACCAGACCATGAG
Mouse-lfit1	TACAGGCTGGAGTGTGCTGAGA	CTCCACTTTTCAGAGCCTTCGCA
Mouse-lfit3	GCTCAGGCTTACGTTGACAAGG	CTTTAGGCGTGTCCATCCTTCC
Mouse-mtDNA Dloop1	AATCTACCATCCTCCGTGAAACC	TCAGTTTAGCTACCCCCAAGTTT AA
Mouse-mtDNA Dloop2	CCCTTCCCATTTGGTCT	TGGTTTCACGGAGGATGG
Mouse-mtDNA Dloop3	TCCTCCGTGAAACCAACAA	AGCGAGAAGAGGGGCATT
Mouse-mtDNA Cytb	GCTTTCCACTTCATCTTACCATTTA	TGTTGGGTTGTTTGATCCTG
Mouse-mtDNA ND1	CTAGCAGAAACAACCGGGC	CCGGCTGCGTATTCTACGTT
Mouse-mtDNA ND4	AACGGATCCACAGCCGTA	AGTCCTCGGGCCATGATT
Mouse-nucDNA Tert	CTAGCTCATGTGTCAAGACCCTCT T	GCCAGCACGTTTCTCTCGTT
Mouse-Cad	CTGCCCGGATTGATTGATGTC	GGTATTAGGCATAGCACAAACC A
Mouse-Vdac1	CCCACATACGCCGATCTTGG	GTGGTTTCCGTGTTGGCAGA
Mouse-Vdac3	CAAAGGGTATGGGTTTGGCAT	TTGGTCTCTAGGTTGCCTGAT
Mouse-Got2	GGACCTCCAGATCCCATCCT	GGTTTTCCGTTATCATCCCGGTA
Mouse-Gpt2	AACCATTCACTGAGGTAATCCGA	GGGCTGTTTAGTAGGTTTGGGT A
Human-ACTB	TCCCTGGAGAAGAGCTACG	GTAGTTTCGTGGATGCCACA
Human-IFNB	AGGACAGGATGAACTTTGAC	TGATAGACATTAGCCAGGAG
Human-CXCL10	TGGCATTCAAGGAGTACCTC	TTGTAGCAATGATCTCAACACG
Human-CCL5	GCTGTCATCCTCATTGCTACTG	TGGTGTAGAAATACTCCTTGATG TG
Human-ISG54	CTGAACCGAGCCCTGCCGAAC	GCTGCCTCGTTTTGCCCTTTGA G

407

408

409

410

411

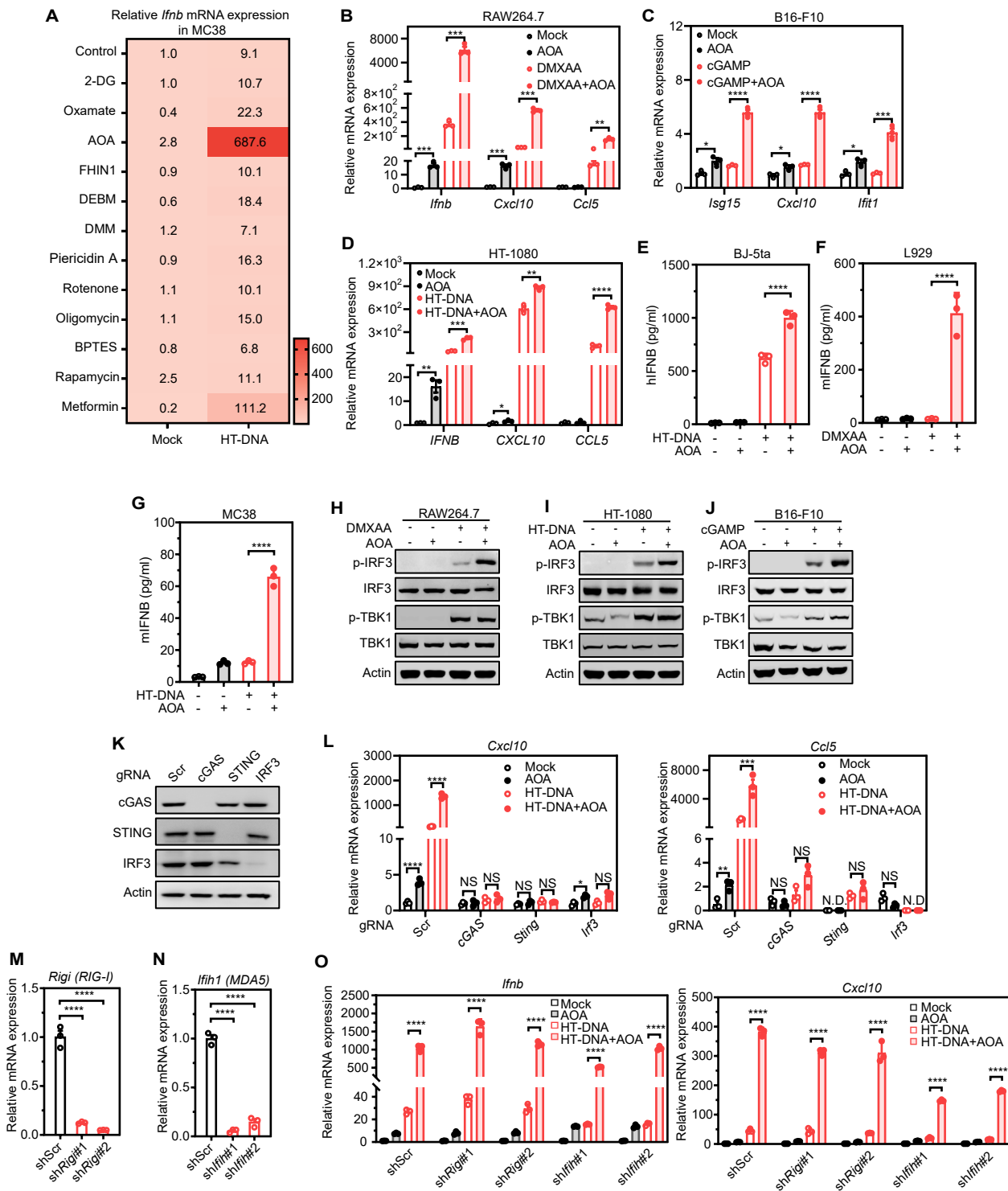
Table S2: sgRNA and shRNA oligos used in this paper

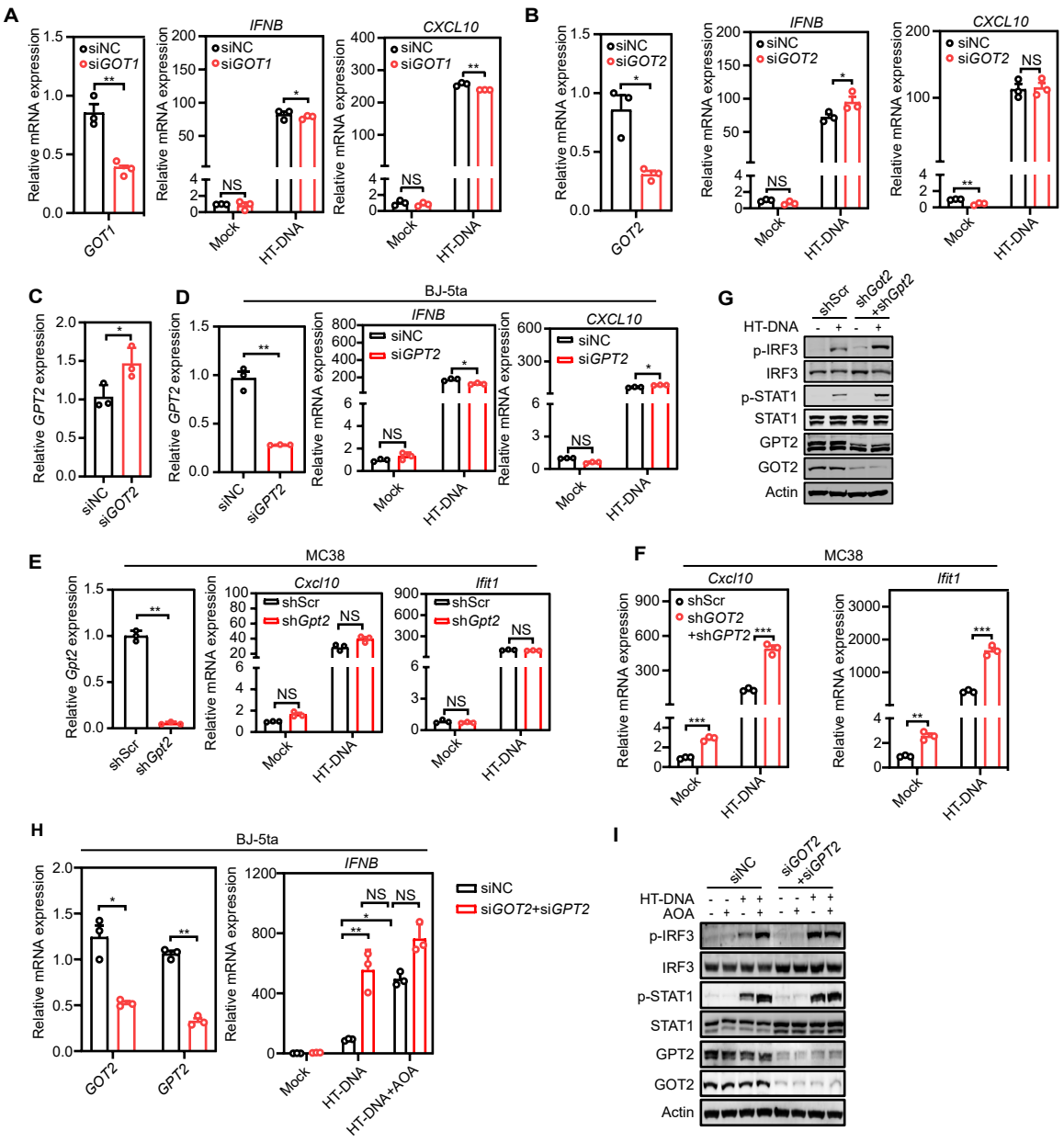
Gene	Sequence	Comments
<i>Cad-1</i>	CCGAGTCTTGCTGAACCTAA	shRNA
<i>Cad-2</i>	GCCTCCACGAAAGGTTCTAAT	shRNA
<i>Vdac1</i>	GAGTTGATAAATACCACGTTA	shRNA
<i>Ripk1</i>	CCTGAATGACATCAATGCAAA	shRNA
<i>Ripk3</i>	GCTATGGTTAATCTTCGTAAT	shRNA
<i>Mkl-1</i>	GCAGGATTTGAGTTAAGCAAA	shRNA
<i>Mkl-2</i>	CGGACAGCAAAGAGCACTAAA	shRNA
<i>Rigi-1</i>	CCACAGTTGATCCAAATGATA	shRNA
<i>Rigi-2</i>	ACTGGAACAGGTCGTTTATAA	shRNA
<i>Ifih1-1</i>	CCACAGAATCAGACACAAGTT	shRNA
<i>Ifih1-2</i>	CTACAAATCAACGACACGAT	shRNA
<i>Vdac3</i>	CGAGAGGATTGAAACGTCAAT	shRNA
<i>Cgas</i>	ATATTCTTGCTAGCTCAATCC	sgRNA
<i>Sting</i>	GAAGGCCAAACATCCAACCTG	sgRNA
<i>Irf3</i>	CCAGTGGTGCCTACACCCCG	sgRNA
<i>Bax</i>	GTTTCATCCAGGATCGAGCA	sgRNA
<i>Bak</i>	GGAACTCTGTGTCGTAGCGC	sgRNA
<i>Zbp1-1</i>	GAAGATCTACCACTCACGTC	sgRNA
<i>Zbp1-2</i>	AGTCCTTTACCGCCTGAAGA	sgRNA

412

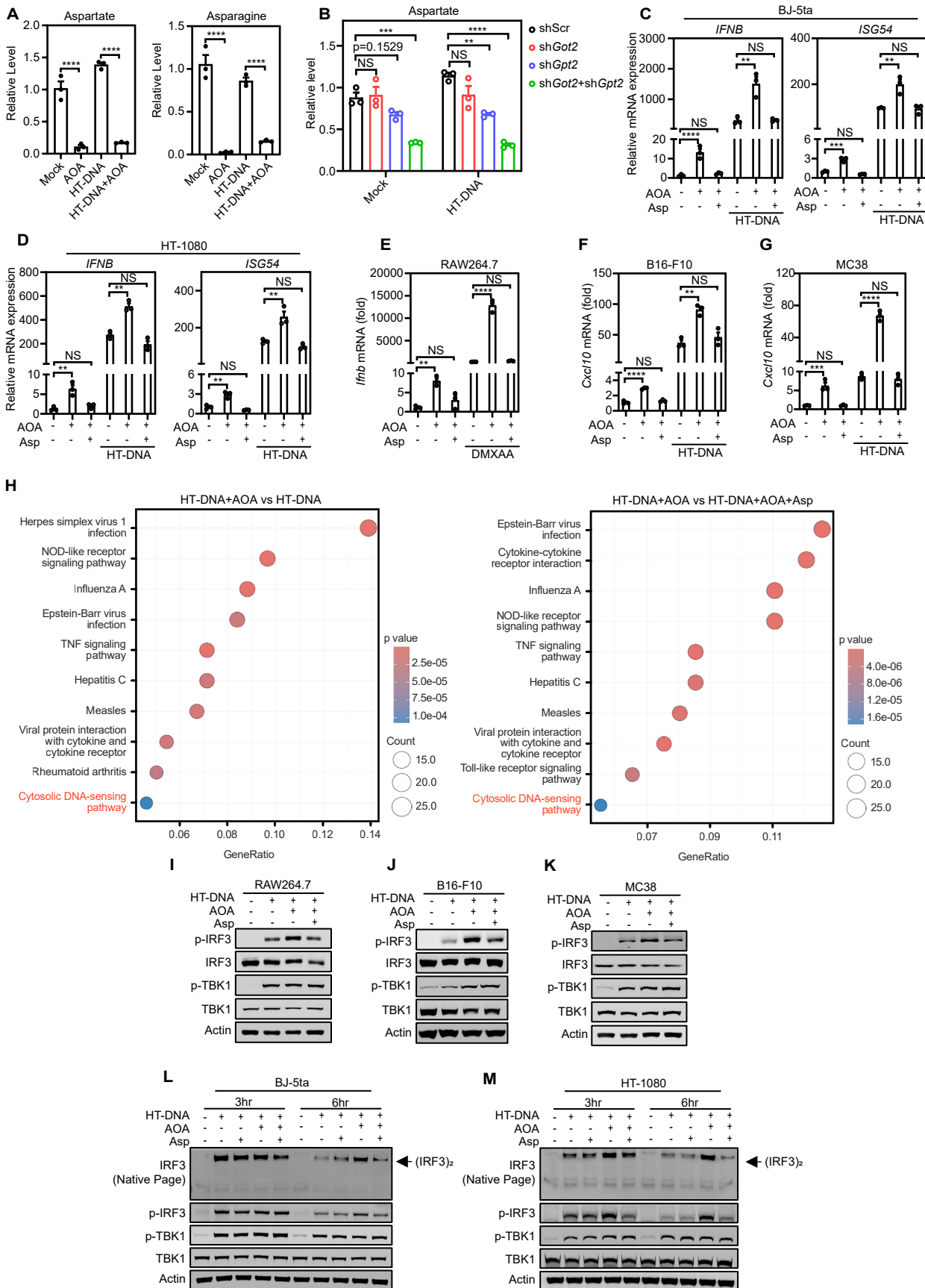
413

Supplemental Figure 1



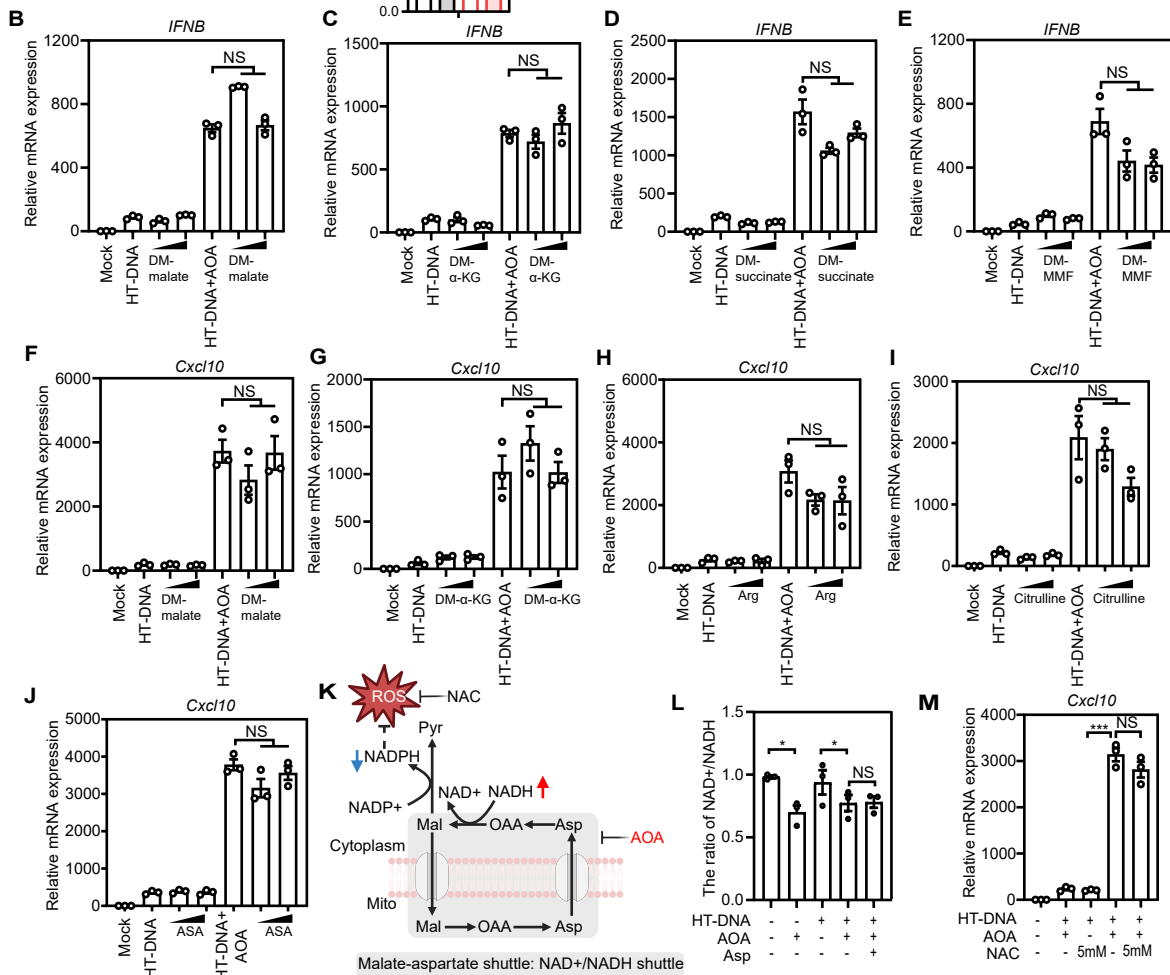
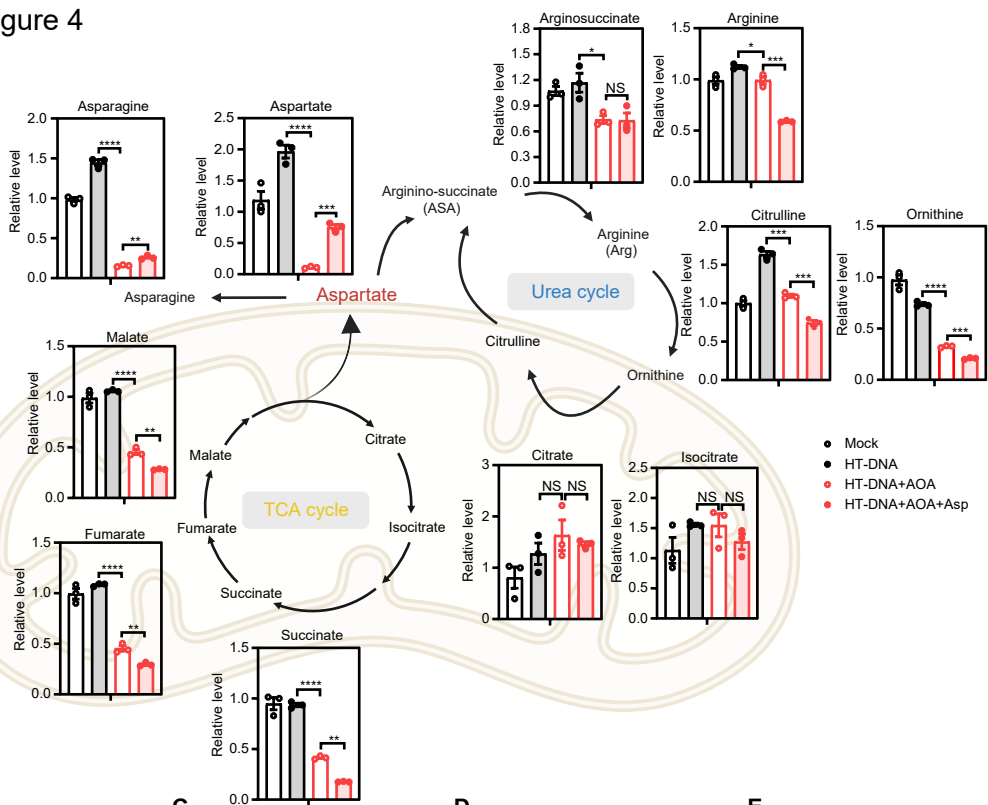


Supplemental Figure 3

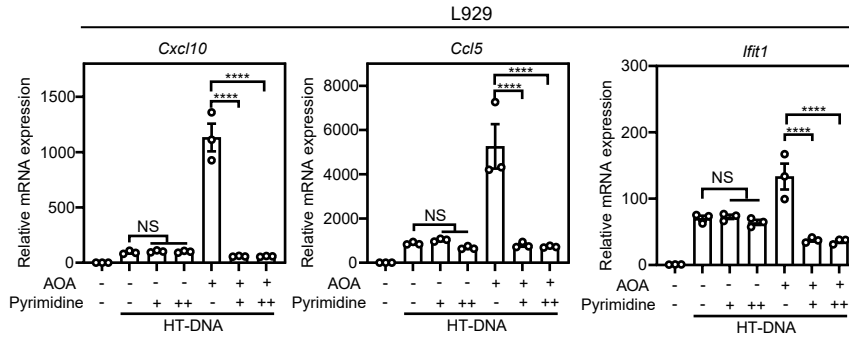


Supplemental Figure 4

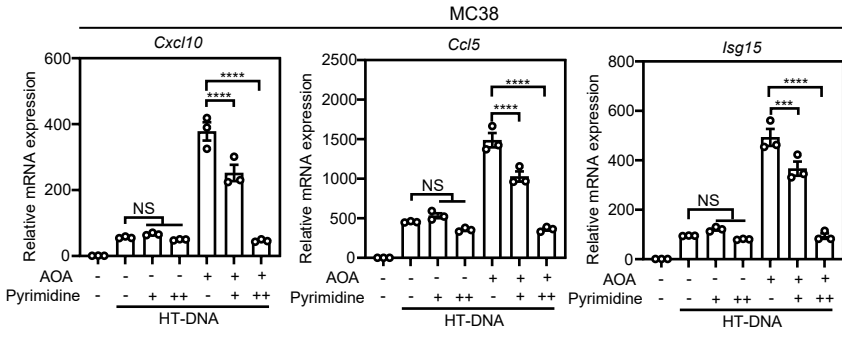
A



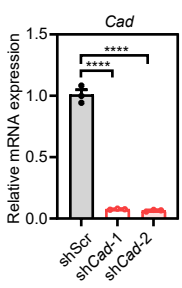
A



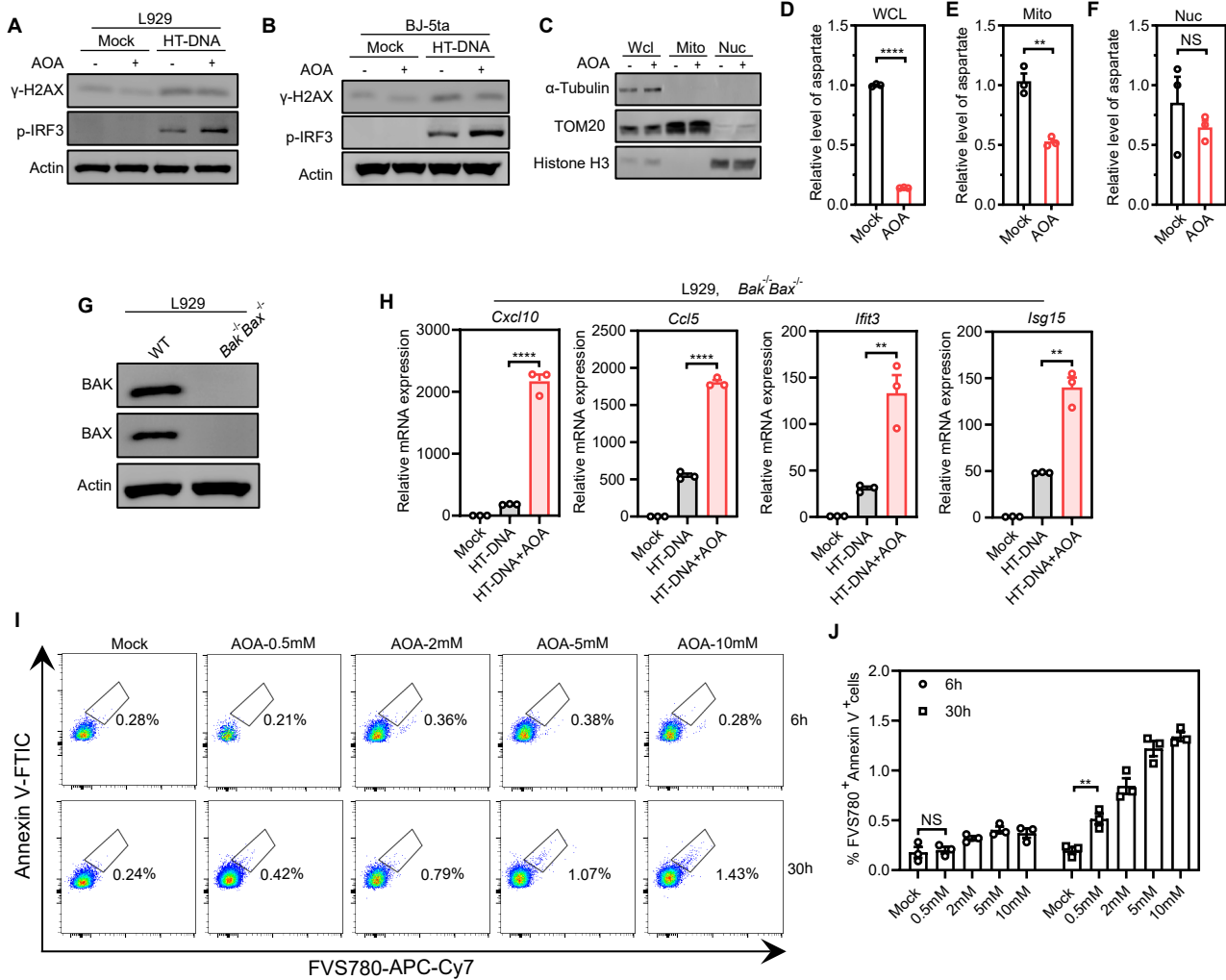
B



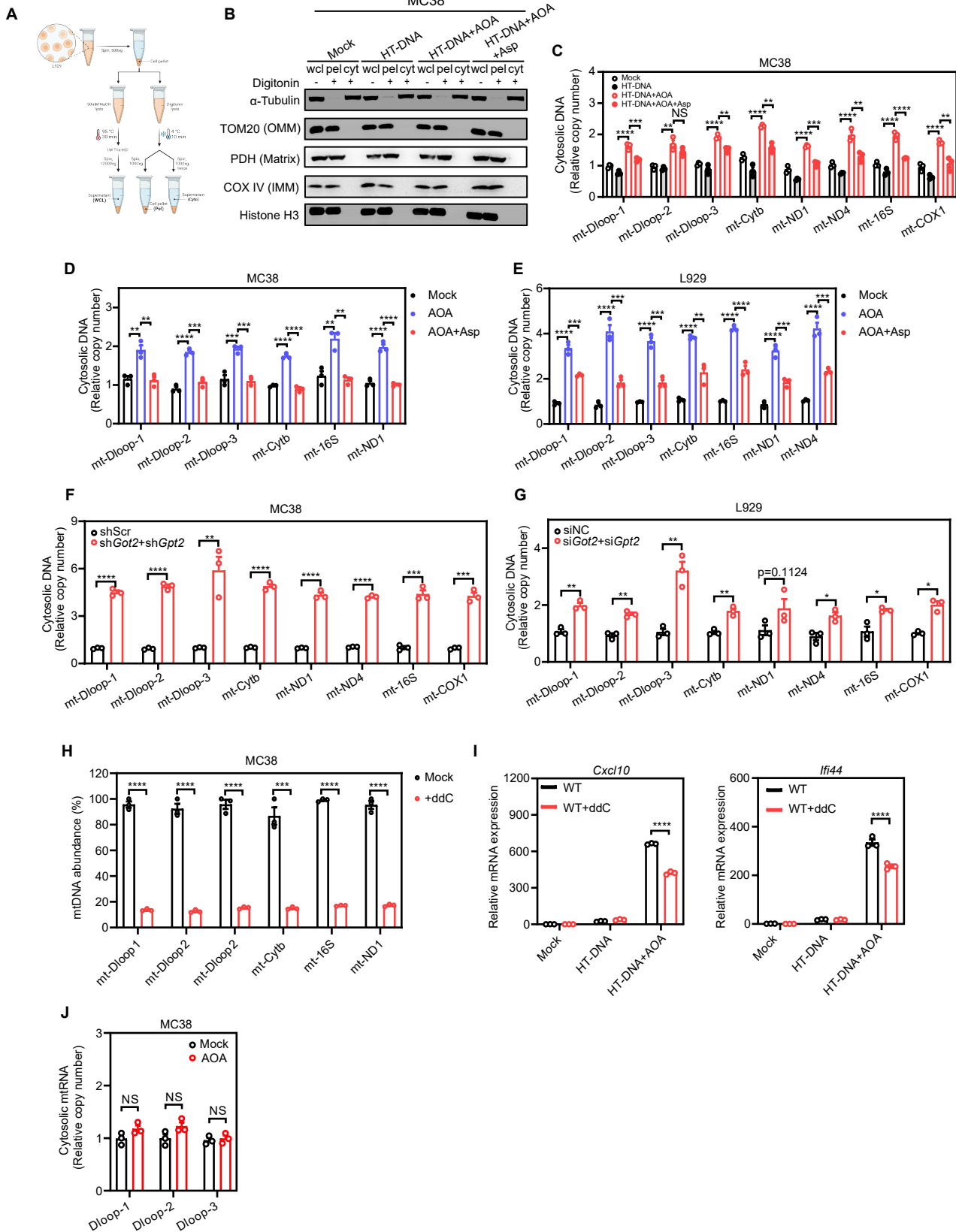
C

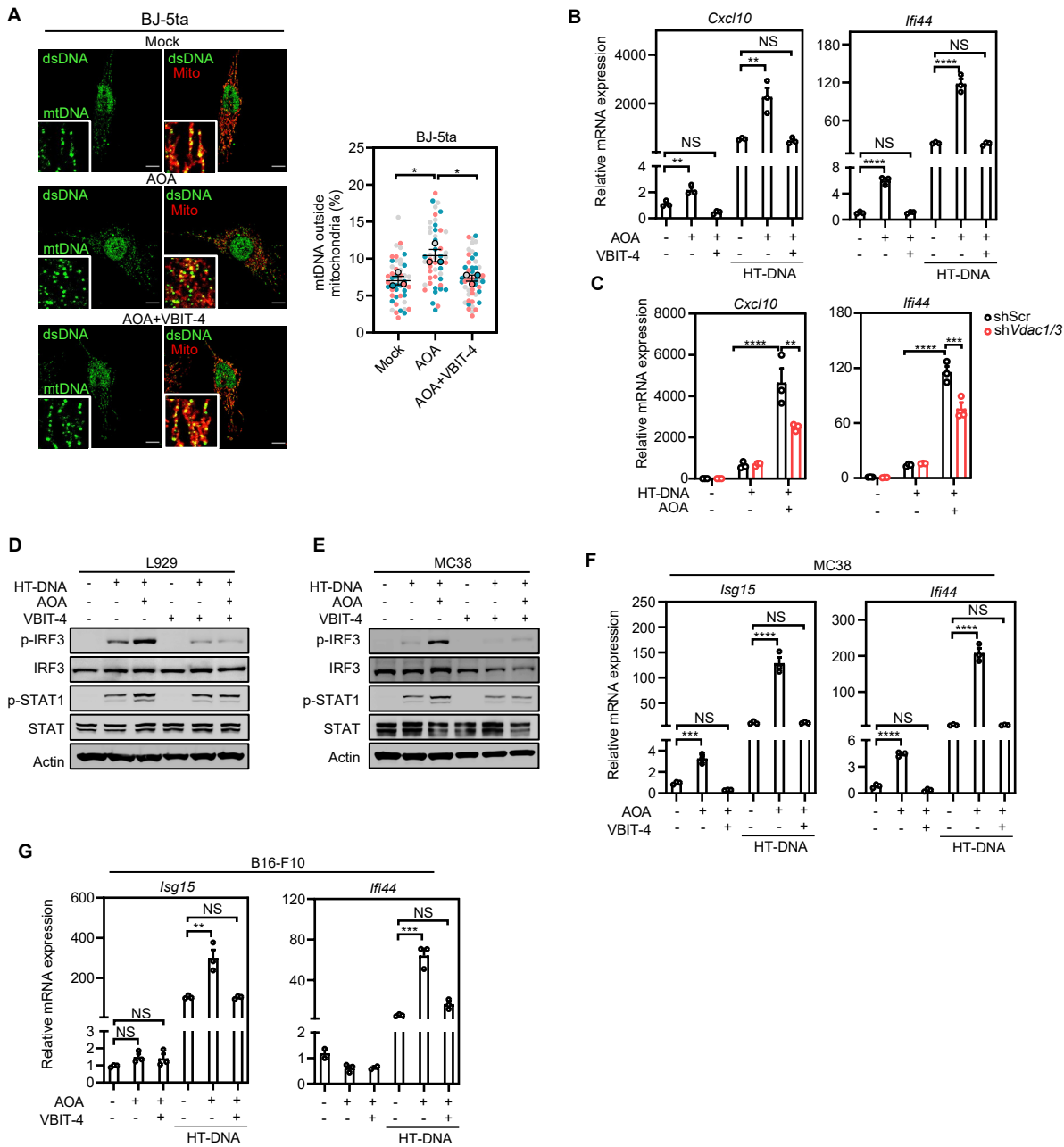


Supplemental Figure 6

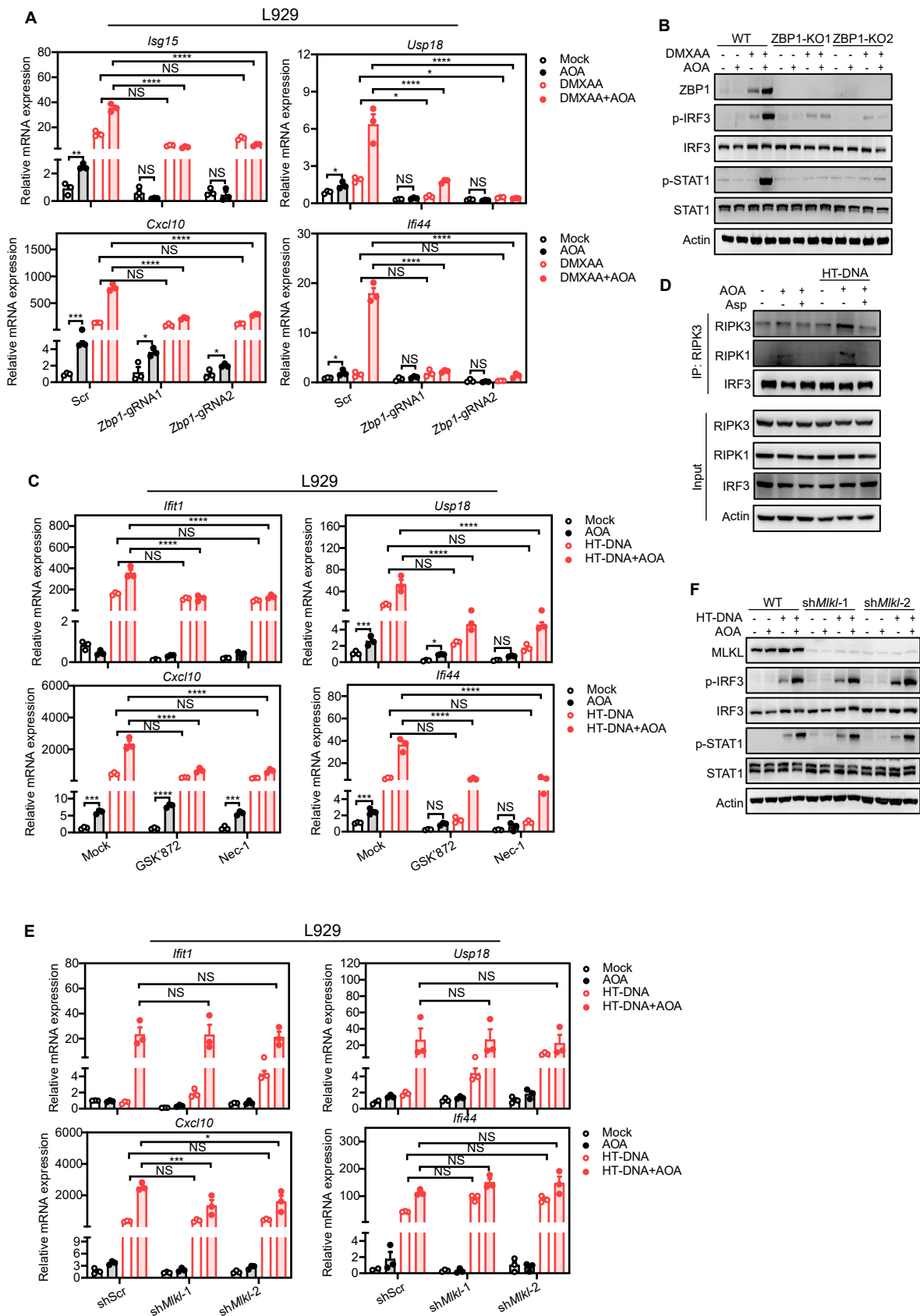


Supplemental Figure 7

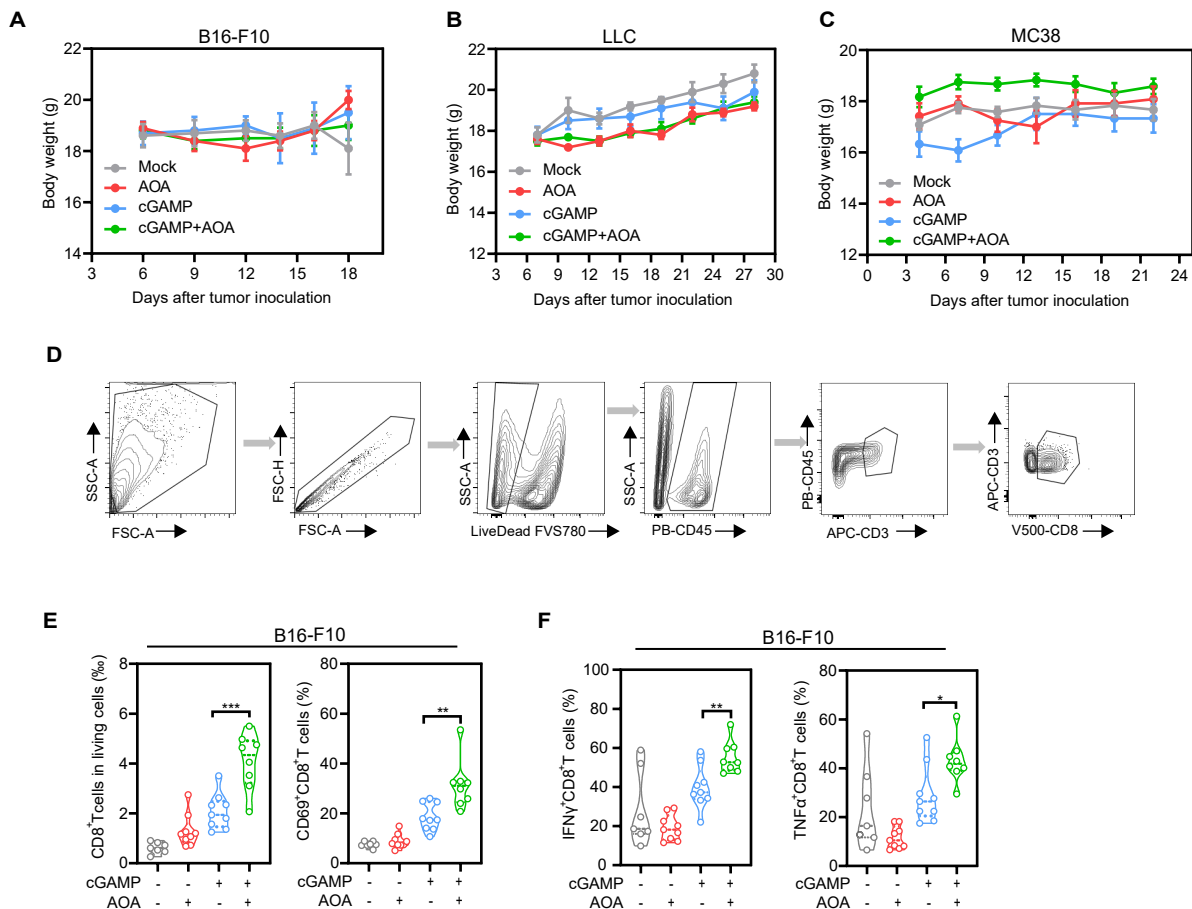




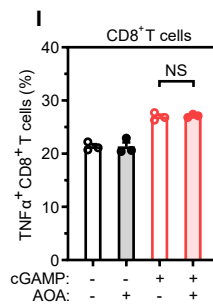
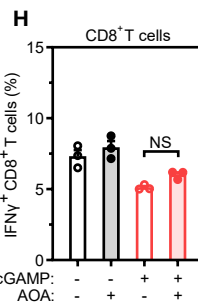
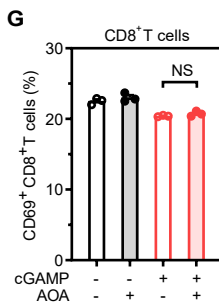
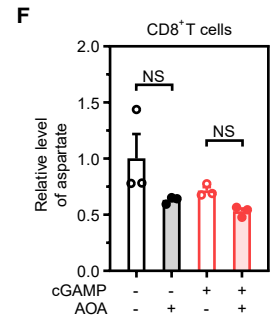
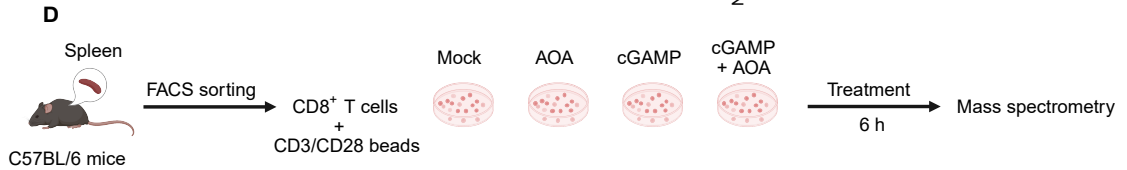
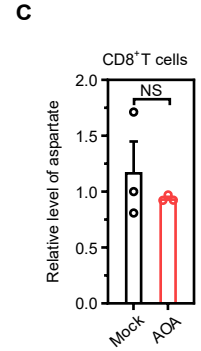
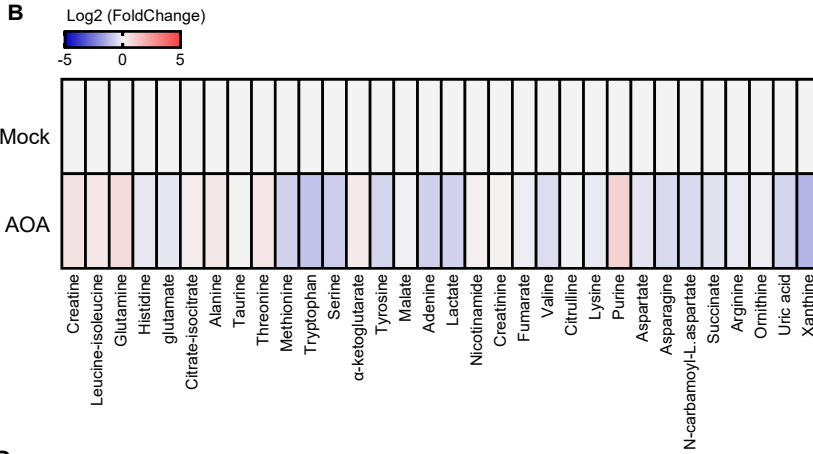
Supplemental Figure 9



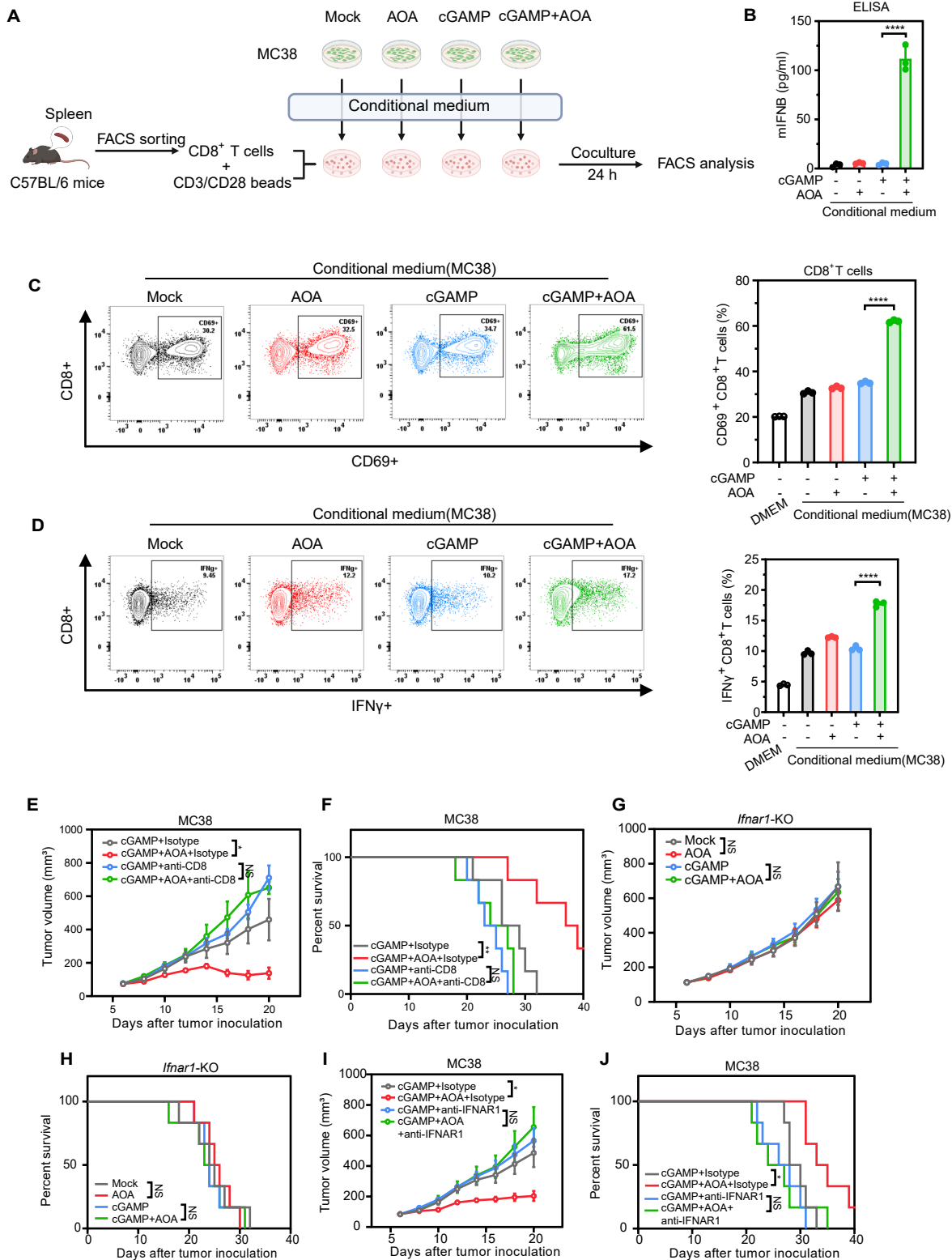
Supplemental Figure 10



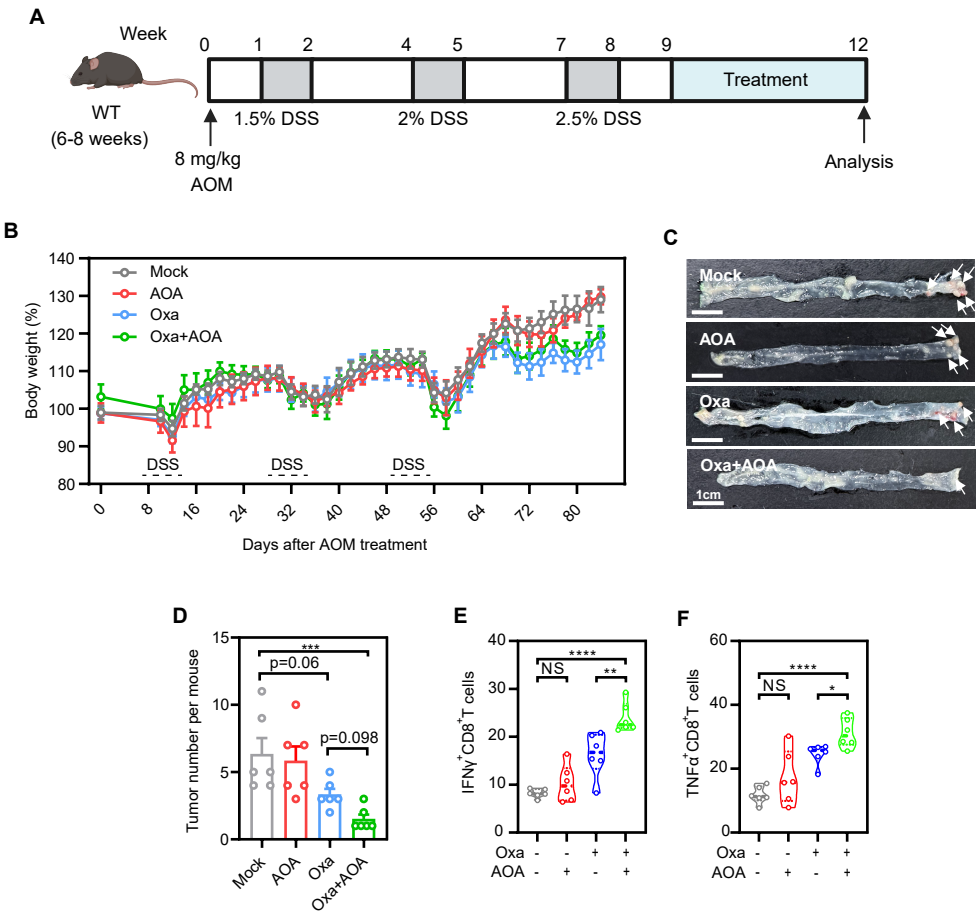
Supplemental Figure 11



Supplemental Figure 12



Supplemental Figure 13



Supplemental Figure 14

